Structure, Volume *26*

Supplemental Information

Structure of an RNA Aptamer that Can Inhibit HIV-1 by Blocking Rev-Cognate RNA (RRE) Binding and Rev-Rev Association

Altaira D. Dearborn, Elif Eren, Norman R. Watts, Ira W. Palmer, Joshua D. Kaufman, Alasdair C. Steven, and Paul T. Wingfield

Figure S1

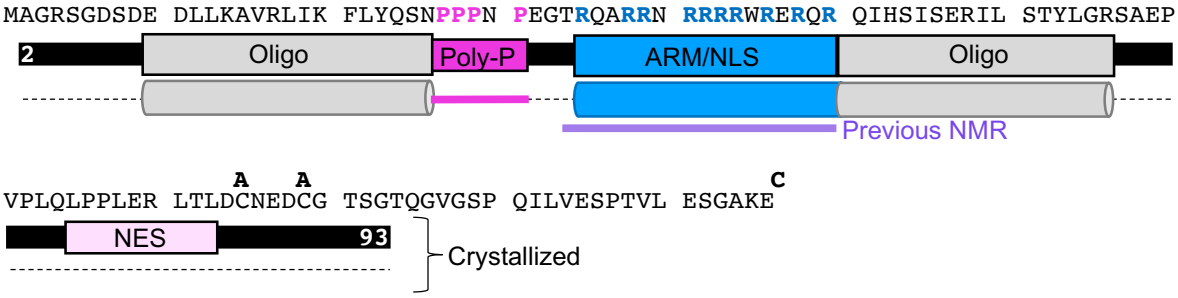

Figure S1. Related to Figure 1. Schematic representations of Rev. (A) Rev^{116} sequence (top line) with mutations made for SPR (above sequence). Arginine residues (blue) in the ARM, and prolines in the poly-proline motif (dark pink) are noted. Rev^{93} functional regions (second line) and secondary structure (third line) includes the Oligomerization motifs (gray), Poly-Proline motif (dark pink), the ARM that overlaps the NLS (blue), and the NES (pale pink). 16-residue ARM peptide from previous NMR is denoted by a purple line (bottom).

Figure S2

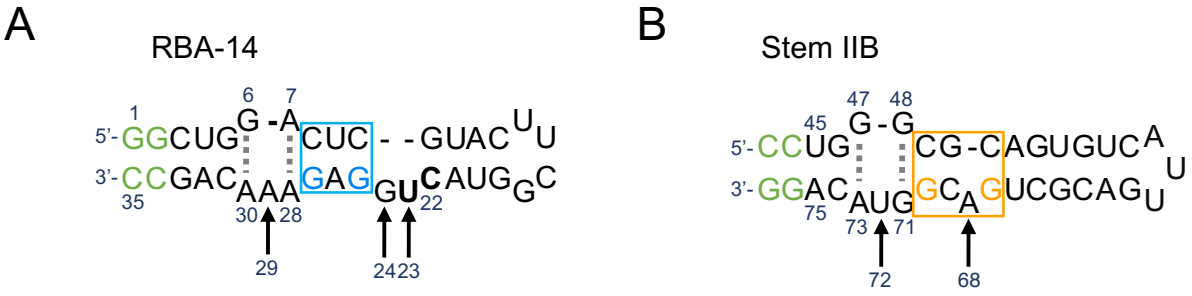

Figure S2. Related to Figure 2. Synthetic RNA with the (A) RBA-14 and (B) Stem IIB sequences. (A and B) GC-clamps are colored green and arrows indicate bulge bases. Purine-purine base-pairs that widen the major groove are indicated by dotted lines and adjacent duplex (blue and orange boxes). Bases that stack with (bold) and those that hydrogen bond with (blue or orange) guanidinium groups from Rev Arg35 and Arg39. (B) Numbering is based on the complete RRE (Foley et al., 2017).

Figure S3

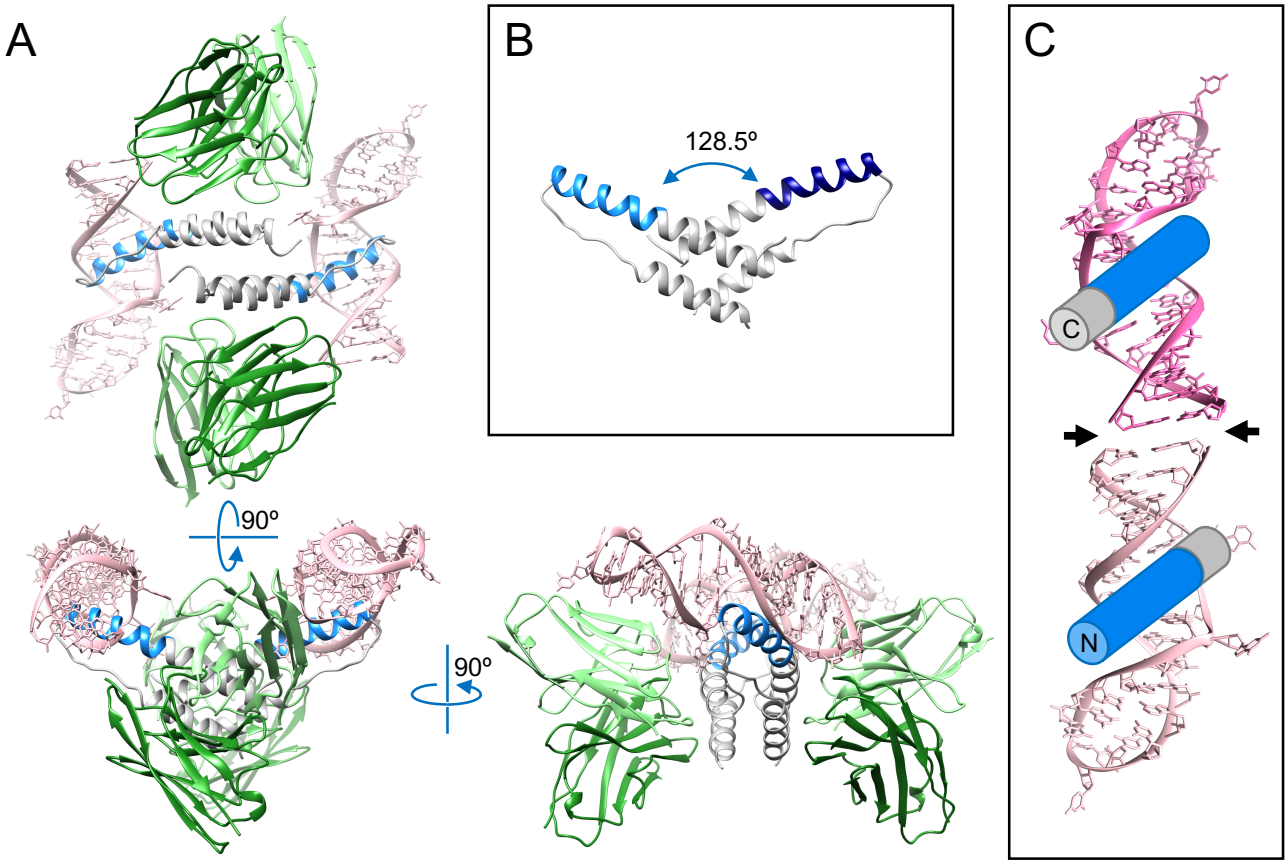

Figure S3. Related to Figure 3. Crystal contacts of the Rev^{93}:scFv:RBA-14 ternary complex. (A) Top and side views of two asymmetric units showing the dimerization of Rev (gray/blue) while bound to RBA-14 (pink) and the scFv (green). (B) The A-A dimer of Rev (gray/blue) forms a 128.5º angle between oligomerization domains (gray). (C) Two molecules of RBA-14 (pink and dark pink) stacking end to end (arrows). The ARM of Rev (blue cylinder) is located in the major groove of RBA-14, part of the adjacent oligomerization helix (gray cylinder) indicates directionality.

Figure S4

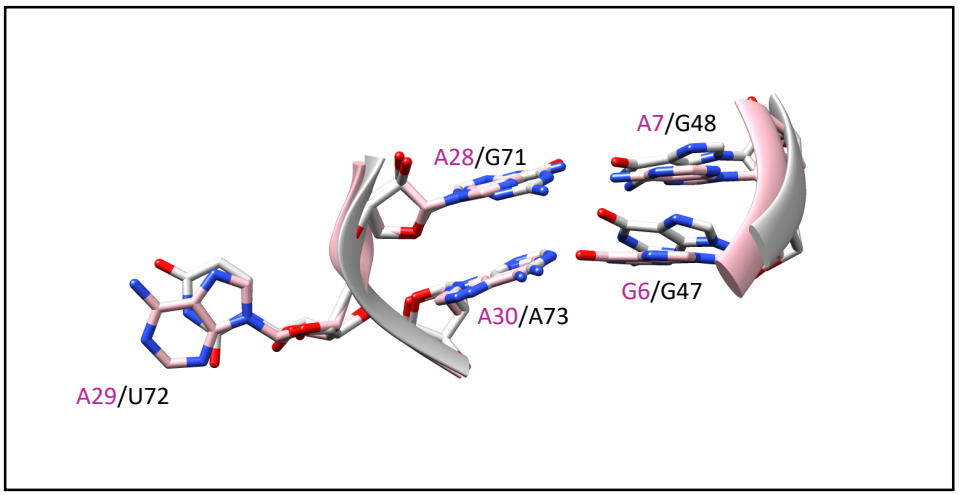

Figure S4. Related to Figure 4. Comparison of purine-purine base pairs in RBA-14 (pink) and Stem IIB (white). Bases are labeled RBA-14 (pink) and Stem IIB (black).

Figure S5

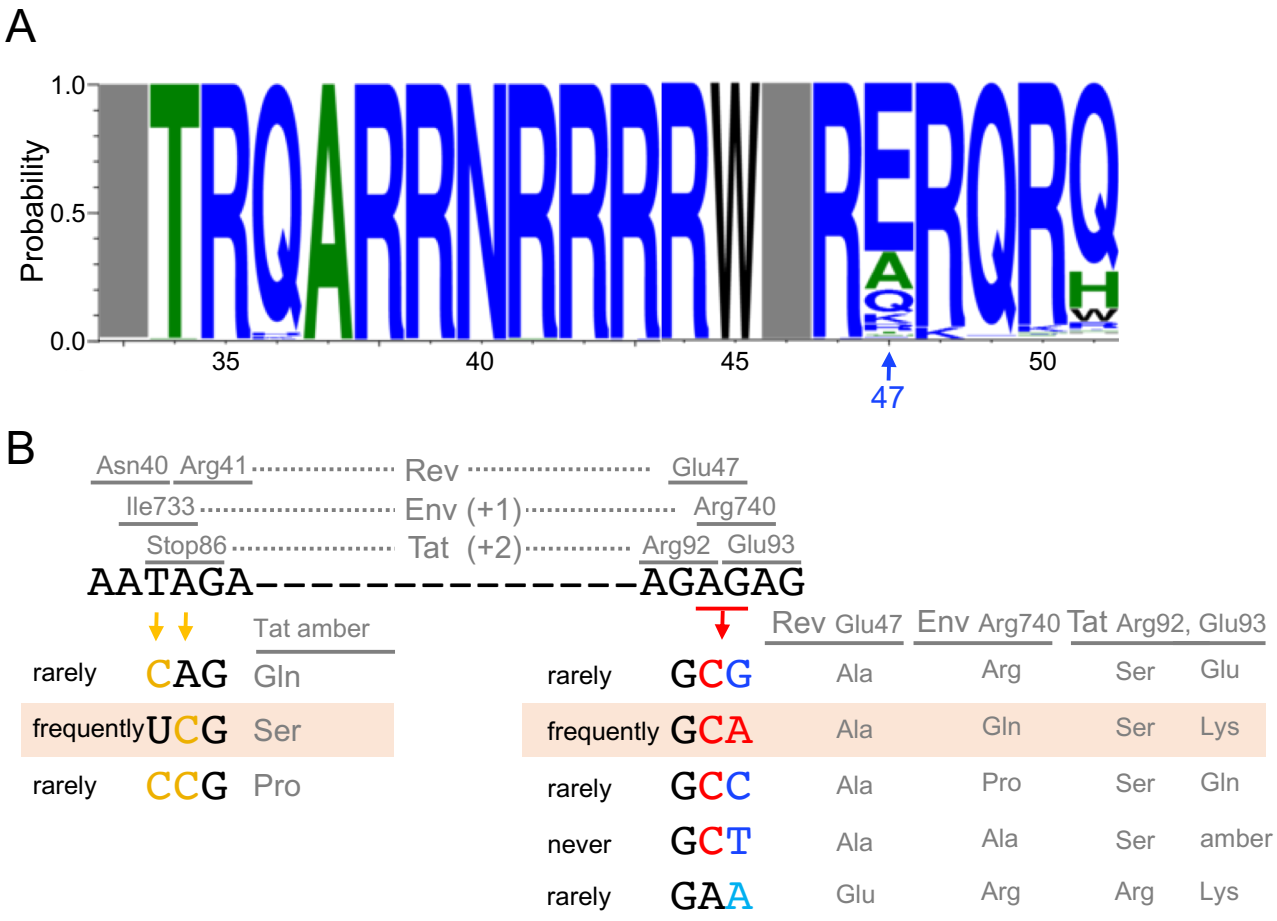

Figure S5. Related to Figure 5. Viral isolate sequence variation. (A) Consensus sequence of Rev residues 34-51 from HIV-1 subtype-B viral isolates, corresponding to the ARM/NLS in Figure S1A (Foley et al., 2017). (B) Proviral DNA sequence of interest (nucleotides 8420-8445 in reference sequence HXB2), intervening nucleotides are indicated by dashes and translation of overlapping reading-frames are annotated above (gray). Missense mutation of the tat amber stop at codon 86 is common (yellow) and produces Tat^{100}. These mutations are silent in Rev and the most frequent mutation (highlighted) is silent in Env. Outside of subtype-B, rev frequently has a double mutation (red) that encodes Rev (Glu47Ala) and also affects Env and Tat (highlighted) in overlapping reading-frames. Wobble-base variants of the alanine codon (blue) and glutamate codon (cyan) are rare despite a higher probability of single point mutation. Together, these observations indicate that the preference for the double-mutant that gives rise to Rev (Glu47Ala) is derived from evolutionary pressure on Env or Tat (gray).

Figure S6

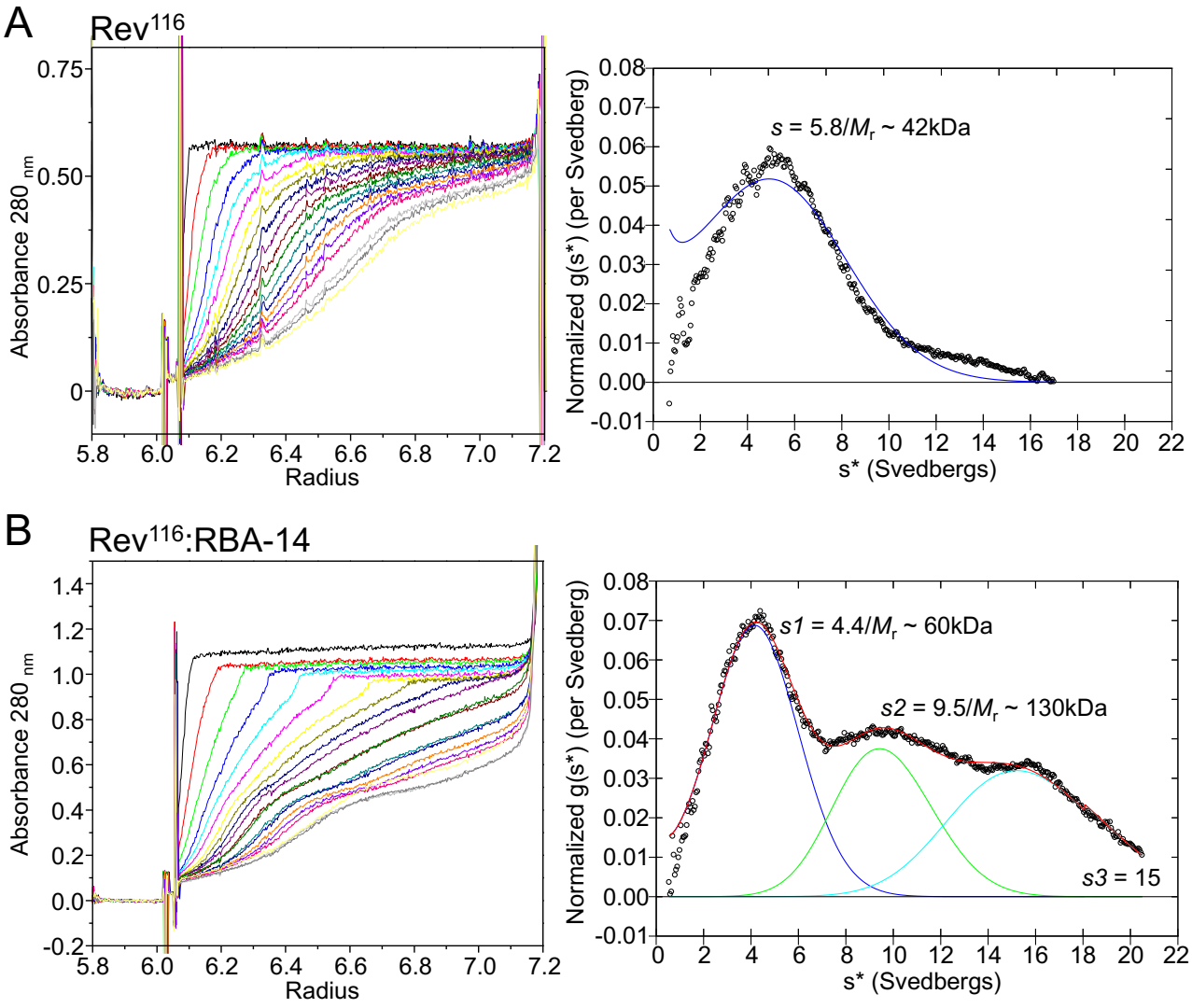

Figure S6. Related to Figure 6. Assembly state of Rev^{116} and Rev^{116}:RBA-14. Sedimentation velocity analysis (left) and size distribution plots (right) of (A) Rev^{116} and (B) Rev^{116}:RBA-14, corresponding to samples in Figure 6B, black and green lines, respectively. Sedimentation velocity analyses show scans at 8-minute intervals, where the direction of sedimentation is from left to right. The species distribution plots were determined using DCDT+ analysis and indicate the sedimentation coefficients (s) where s stands for svedbergs which have units of 10-13 seconds. The approximate molecular weights of the resolved species are also indicated.

Figure S7

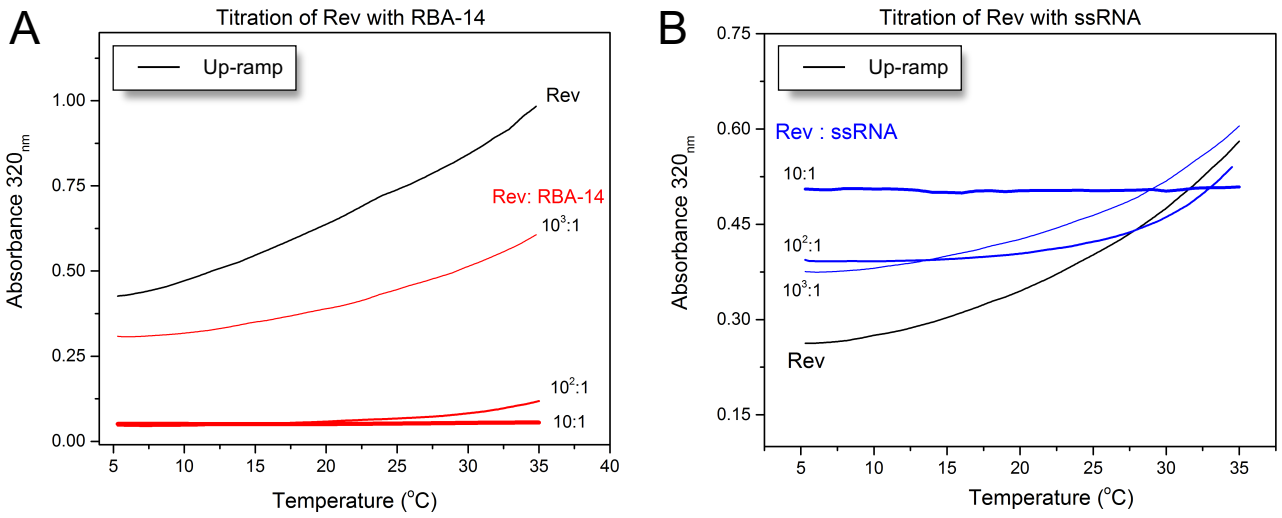

Figure S7. Related to Figure 6. Disassembly of Rev^{116} by RBA-14 but not ssRNA. A_{320} light scatter of Rev on third up-ramp of three thermal cycles for each concentration in these series. Rev was titrated with increasing molar ratios (increasingly thicker lines) of (A) RBA-14 and (B) 30-nt ssRNA at 5 °C, thermally cycling three times to 35 °C between each addition to amplify assembly. For each concentration, only the up-ramp is shown.

Table S1. Related to Figure 2. Kinetics/Affinity calculations from Surface Plasmon Resonance

Analyte	**Signal Max. (RU)**	**Fitting Model**	**Residuals Limit**	**k_a1 ($M^{-1}s^{-1}$)** $x10^5$	**k_d1 (s^{-1})** $x10^{-3}$	**k_a2 (s^{-1})** $x10^{-3}$	**k_d2 (s^{-1})** $x10^{-3}$	**K_d (M)** $x10^{-9}$
RBA-14	300	1:1 binding	< 35 RU (12%)	4.35	1.54	na	na	3.5
		Two-state	< 20 RU (7%)	3.78	14.1	9.99	1.86	5.8
Stem IIB	225	1:1 binding	< 25 RU (11%)	2.55	1.79	na	na	7.0
		Two-state	< 12 RU (5%)	2.47	21.8	16.6	2.84	12.9
1:1 binding								

$$A + B \underset{k_d1}{\overset{k_a1}{\rightleftharpoons}} AB$$

Two-state

$$A + B \underset{k_d1}{\overset{k_a1}{\rightleftharpoons}} AB \underset{k_d2}{\overset{k_a2}{\rightleftharpoons}} AB^*$$

Table S2. Related to Figure 4. Interface analysis.

Parameter	**Rev:RBA-14**	**Rev:Stem IIB** PDB ID 4PMI
Interface Area (A^2)	819.4	853.6
Hydrogen bonds	**22**	**25**
	Thr34(OG1) : G6(OP1)	Thr34(OG1) : G47(OP2)
	Arg35(NH1) : U23(OP2)	
	Arg35(NH1) : U23(O5')	
	Arg35(NH2) : G25(N7)	Arg35(NH1) : G67(N7)
	Arg35(NH2) : G25(O6)	Arg35(NH1) : G67(O6)
	Gln36(NE2) : A7(OP2)	
		Ala37(N) : G46(O2')
	Arg38(NH1) : C22(OP1)	
	Arg38(NH2) : C22(OP1)	Arg38(NH2) : U66(OP1)
		Arg38(NH1) : G67(OP1)
	Arg38(NH1) : U23(OP2)	Arg38(NH2) : G67(OP2)
		Arg38(NH1) : G67(OP2)
	Arg39(NH2) : G27(O6)	Arg39(NH1) : G70(O6)
	Arg39(NH2) : G27(N7)	Arg39(NH2) : G70(N7)
	Arg39(NH1) : A28(O2')	
		Arg39(NH1) : G48(O6)
	Asn40(ND2) : G5(O2')	Asn40(ND2) : G46(O2')
	Asn40(ND2) : G6(O6)	Asn40(ND2) : G47(O6)
	Asn40(OD1) : A30(N6)	Asn40(OD1) : G71(N2)
	Arg41(NE) : G5(OP2)	Arg41(NE) : U45(OP1)
	Arg41(NH2) : G5(OP1)	Arg41(NH2) : G46(OP2)
		Arg43(NE) : G71(O2')
	Arg43(NH1) : A28(O2')	Arg43(NH2) : G71(O3')
	Arg43(NH1) : A28(O3')	
		Arg43(NH2) : A73(N7)
	Arg44(NH1) : G5(N7)	Arg44(NH1) : G46(N7)
	Arg44(NH2) : U4(OP2)	Arg44(NH1) : G46(O6)
	Arg46(NH2) : A29(OP2)	
		Arg48(NH1) : U43(O3')
		Arg50(NH1) : U72(OP1)
		Arg50(NH2) : U72(O4')
Stacking interactions	**5**	**3**
	Arg35 : C22	Arg35 : U66
	Arg35 : U23	
	Arg39 : U23	Arg39 : C69
	Arg44 : U4	Arg44 : U45
	Arg50 : A29	